Anat. Histol. Embryol. **34,** 215–219 (2005)

ISSN 0340–2096

Departamento de Morfología (Anatomía y Embriología), Facultad de Veterinaria, Universidad de Las Palmas de Gran Canaria, Las Palmas de Gran Canaria, Spain

Normal Anatomical Imaging of the Thorax in Three Dogs: Computed Tomography and Macroscopic Cross Sections with Vascular Injection

M. A. Rivero[1]*, J. A. Ramírez[1], J. M. Vázquez[2], F. Gil[2], G. Ramírez[2] and A. Arencibia[1]

Addresses of authors: [1]Department of Morphology, Faculty of Veterinary, University of Las Palmas de Gran Canaria, Las Palmas de Gran Canaria 35416, Spain; [2]Department of Anatomy, Faculty of Veterinary, University of Murcia, Murcia 30100, Spain; *Corresponding author: Tel.: +34 928 454 352; fax: +34 928 451 141; e-mail: mrivero@dmor.ulpgc.es

With 7 figures

Received December 2003; accepted for publication August 2004

Summary

The purpose of this study was to provide a new reference for interpretation of the normal anatomy of the canine thorax as imaged using computed tomography (CT). Three mature dogs, all mixed breed males, were used for this study. The dogs were sedated, anaesthetized and maintained in sternal recumbency. CT study from the first to the thirteen thoracic vertebra was performed with a TOSHIBA 600HQ scanner (third generation equipment). Dogs were killed and vascular-injection technique was performed: red latex and blue latex filled vascular system. Injected dogs were frozen and sectioned with an electric bandsaw, the cuts matched as closely as possible to the CT images. The CT images from this study are intended as a reference for clinical CT imaging studies of the thoracic cavity of the dog and for interpreting lesions of the thorax and associated structures.

Introduction

During the last two decades, computed tomography (CT) has become an useful diagnostic tool (Samii et al., 1998). Because of its limited accessibility and high costs, it was not initially used in veterinary medicine; however, accessibility has improved, which has increased the need for expertise in the use of this technique in animals (Ottesen and Moe, 1998). Its use in veterinary medicine has focused on diseases of the thorax and abdomen (Barthez et al., 1998; Ottesen and Moe, 1998) and skeletal disorders (Carpenter et al., 1993; Feeney et al., 1996).

Computed tomography images provide detailed anatomic information that is difficult to obtain with other diagnostic techniques (Schwarz and Tidwell, 1999). CT produces images of thin cross-sections, which can be reconstructed as multiplanar images by the computer (Feeney et al., 1991; Ottesen and Moe, 1998). Accurate interpretation and identification of CT images requires a thorough knowledge of the planimetric anatomy and its topography (Feeney et al., 1991; Smallwood and George, 1993; Samii et al., 1998).

Although other authors have addressed cross-sectional anatomy of the thorax using CT and other techniques (Feeney et al., 1991; Smallwood and George, 1993; Assheuer and Sager, 1997), we believe that our work includes additional information by providing a better quality of CT images and comparing them with anatomical specimens that have been vascularly injected for a better definition of the morphology and topography of the vascular structures.

Computed tomography is becoming increasingly important in the diagnosis and evaluation of thoracic disease such as pulmonary, thoracic wall and mediastinal masses, pneumothorax and pleural fluids (Burk, 1991; Smallwood and George, 1993; Ottesen and Moe, 1998; Spann et al., 1998; Waters et al., 1998; Schwarz and Tidwell, 1999).

Materials and Methods

Three mature dogs, all mixed breed males, were used for this study. Their weight ranged 25–34 kg and their average height was 60 cm. The dogs were sedated with 0.2 mg/kg of acepromazine (Calmo Neosan; Pfizer, New York, NY, USA) and anaesthetized with 15 mg/kg i.v. of pentobarbital sodium (Braun; Braun Medical, Melsungen, Germany). Throughout the procedure, the animals were maintained in sternal recumbency perpendicular to exploration table. CT study was performed at the Radiodiagnostic Service of the Hospital Universitario Insular of Las Palmas de Gran Canaria with a TOSHIBA 600HQ scanner (third generation equipment, Toshiba Medical Imaging Systems, Tustin, CA, USA). Transverse slices from the first to the 13 thoracic vertebra were obtained using the following parameters: caudal vision of image (V.V.F.), 8-s exposure time, 120 kV, 80 mA, 10 mm slice thickness. Best image quality for soft tissue was obtained by adjusting window widths and window levels: For soft tissue thorax structures a soft-tissue window was used (WL: 19, WW: 1764).

Immediately following the CT study, the dogs were killed using a barbiturate overdose. The dogs were bled-out with saline solution and latex was injected into their arterial and venous systems: red latex filled systemic arteries and pulmonary veins, whereas the blue latex filled systemic veins and pulmonary arteries. So, the blood vessels were clearly identified.

The injected dogs were frozen at −70°C in the same position that they were scanned within 24 h to minimize post-mortem changes. Once the cadavers were completely frozen, they were sectioned with an electric bandsaw where the cuts matched as closely as possible to the CT images. Each section was 10 mm thick. Sections were cleaned and their caudal surfaces photographed, set of sections were chosen for comparing with their corresponding CT images and with anatomy textbooks (Nickel et al., 1979, 1981; Boyd and Paterson, 1991; Feeney et al., 1991; Ruberte and Sautet, 1996; Done et al., 1997; Dyce et al., 1999; Vázquez et al., 2000). Illustrated Veterinary Anatomical Nomenclature (Schaller, 1992) was used to identify the normal anatomy of the structures of the thorax. Clinically relevant anatomical structures were identified in the anatomic section and in its corresponding CT slice. Although CT and cross-section have approximately the same slice position and orientation, some structures labelled in the CT images could not be identified in its corresponding anatomic cross-section.

Results and Discussion

Clinically relevant anatomic structures were identified and labelled in the two photographs presented in the figures (CT and anatomic section). Fig. 1 is a ventrodorsal radiograph image where the lines depict the CT transverse imaging planes and gross sections (Figs 2–7). These sections are presented in a cranial to caudal progression from the level of first thoracic vertebra (Fig. 2) to the level of heart apex (Fig. 7). CT images and anatomic sections were oriented so that the left side of the thorax is to the viewer's left and dorsal is at the top.

Detailed anatomy of the thorax was acquired with soft-tissue window. Grey scale CT is directly related to the radiation attenuation of the thorax structures. CT images obtained provide a good depiction of bone structures. Thus, the walls and the roof bones of the thorax cavity (rib with its head and tubercle; thoracic vertebrae with their articular and transverse processes, spinous process, vertebral arch and vertebral body), the sternum (manubrium and sternebrae) and, in some images, both scapulas were easily identifiable because of the high CT density and appeared white. In the same way, CT images provided an excellent view of the joint surfaces of costovertebral, costochondral and sternocostal joints. Different muscles (transverse thoracis, longus colli) had an intermediate CT density and appeared grey.

The respiratory system structures (trachea, principal bronchi, both lungs with their lobes) appeared black with a low opacity compared with the tracheal and bronchial cartilages which were observed with an intermediate tissue density. Trachea in the anatomical cross-sections was collapsed.

The vascular system structures (heart with its cavities, thoracic aorta, brachiocephalic trunk, carotid arteries, subclavian arteries, internal thoracic artery and vein, pulmonary vessels, cranial and caudal cava veins, costocervical venous trunk, right azygos vein) were observed grey because they had an intermediate tissue density compared with pericardic fat and thymus that appeared dark grey with a low-intermediate CT density.

Computed tomography is a non-invasive cross-sectional diagnostic imaging technique that offers considerable advantages over traditional radiography. Conventional radiographs depict a three dimensional object as a two dimensional image. Their main limitations are that overlying tissues are superimposed on the image and its inability to distinguish between two tissues with similar density. CT overcomes these problems by scanning thin slices of the body with a narrow X-ray beam, producing an image of each slice as a cross section of the tissues body (Hounsfield, 1973; Collard et al., 1975; Barbee and Allen, 1987; Thrall, 1994; Ottesen and Moe, 1998) and CT can differentiate between tissues of similar density because of the narrow X-ray beam and the use of 'windowing' altering WL and WW. Besides, inferior quality images can be manipulated using the grey scale and compensating their quality. CT provides detailed two-dimensional images with great clarity and better images of bones and soft tissues. CT is more sensitive in detecting diseases, and distinguishes normal

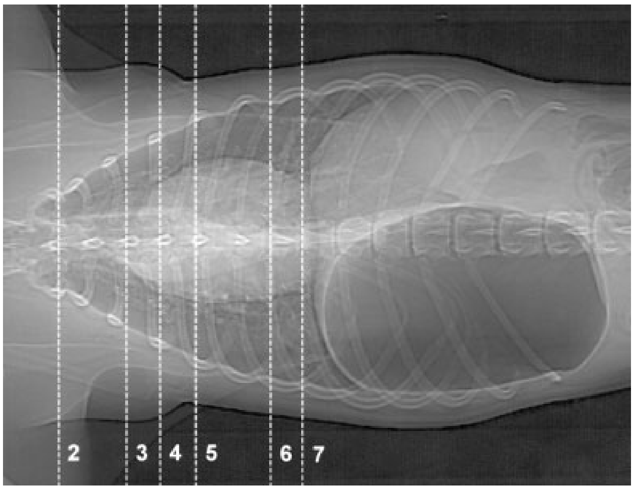

Fig. 1. Dorsal image corresponding to thoracic region. Transverse sections are shown.

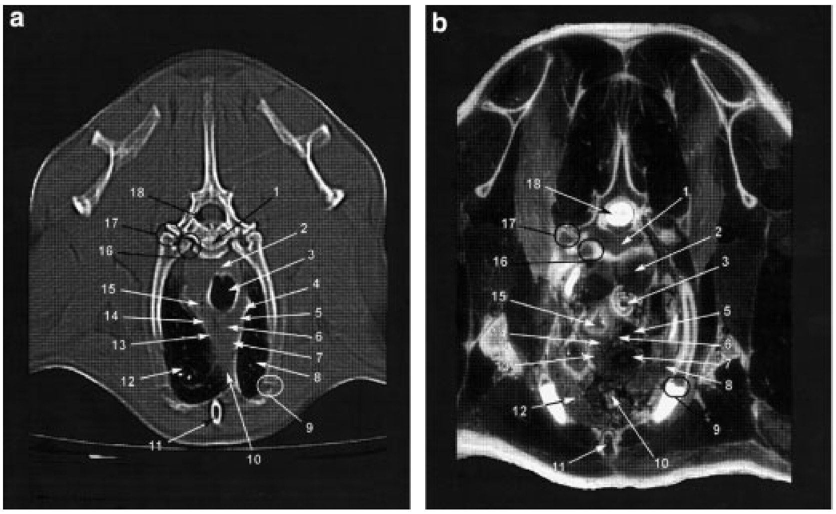

Fig. 2. (a) Computed tomography image and (b) anatomic cross-section at level of first rib. Caudal view. 1, body of first thoracic vertebra; 2, longus colli muscle (thoracic part); 3, trachea: thoracic part; 4, right subclavian artery (only a); 5, brachiocephalic trunk; 6, left common carotid artery; 7, cranial vena cava; 8, right lung: cranial lobe, 9; costochondral joint; 10, thymus; 11, sternum; 12, left lung: cranial lobe; 13, left costocervical venous trunk; 14, left subclavian artery; 15, esophagus: thoracic part; 16, costal head joint; 17, costotransversa joint; 18, spinal cord and epidural fat.

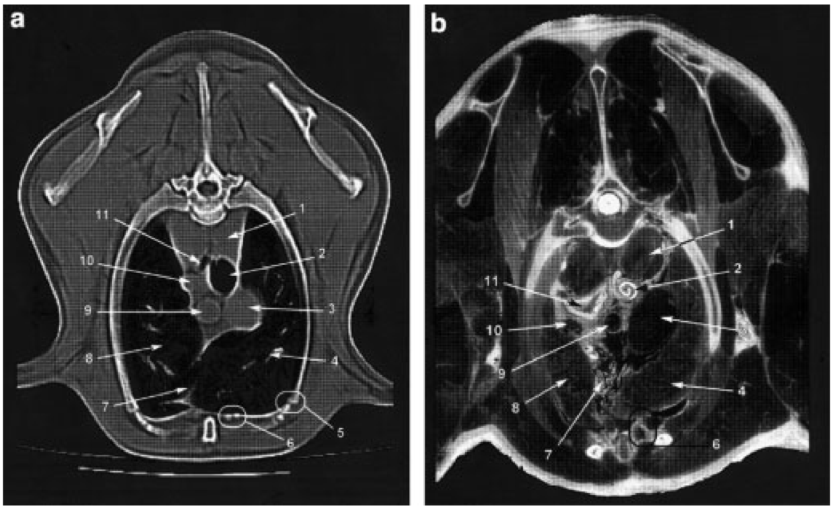

Fig. 3. (a) Computed tomography image and (b) anatomic cross-section at level of third rib. Caudal view. 1, longus colli muscle (thoracic part); 2, trachea: thoracic part; 3, cranial vena cava; 4, right lung: cranial lobe; 5, costochondral joint (only a); 6, internal thoracic artery and vein; 7, cranial mediastinum: thymus; 8, left lung: cranial lobe; 9, brachiocephalic trunk; 10, left subclavian artery; 11, esophagus: thoracic part.

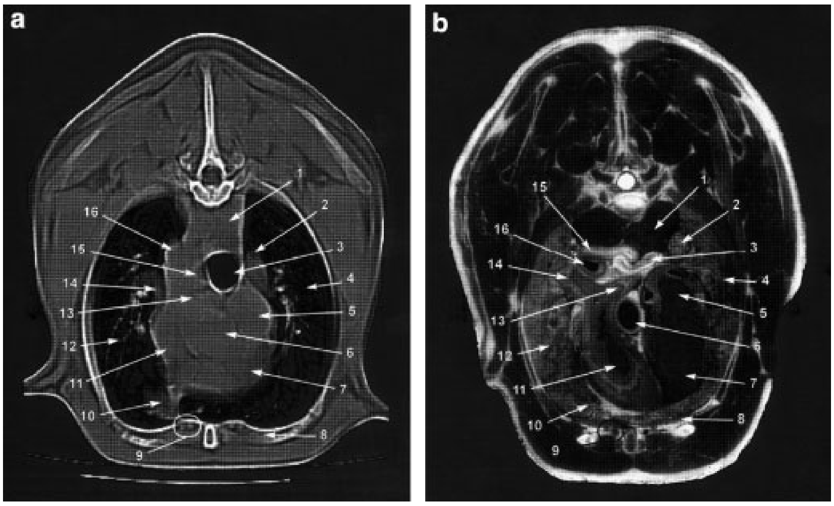

Fig. 4. (a) Computed tomography image and (b) anatomic cross-section at level of right ventricle and pulmonary trunk. Caudal view. 1, longus colli muscle (thoracic part); 2, right azygos vein; 3, trachea: thoracic part; 4, right lung: cranial lobe; 5, cranial vena cava; 6, ascendens aorta; 7, right atrium; 8, transverse thoracis muscle; 9, internal thoracic artery and vein; 10, cranial mediastinum with thymus; 11, right ventricle and pulmonary trunk; 12, left lung: cranial lobe; 13, right pulmonary artery; 14, left pulmonary artery; 15, esophagus: thoracic part; 16, descendens aorta: thoracic aorta.

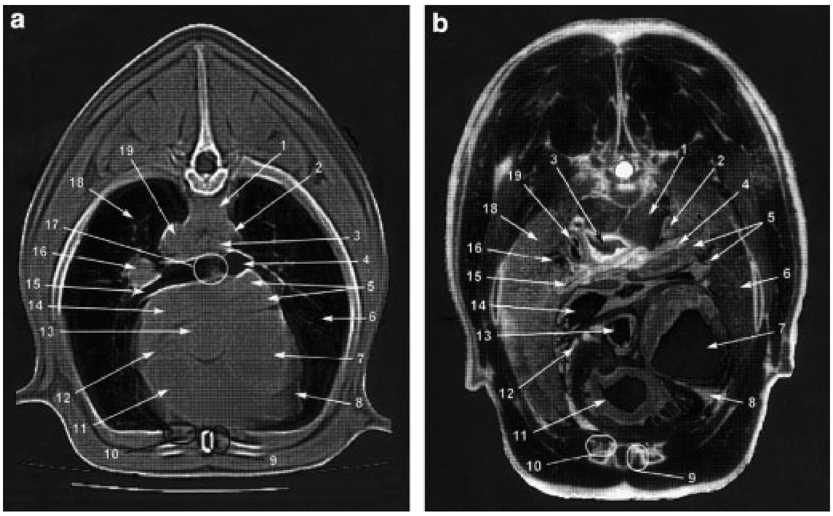

Fig. 5. (a) Computed tomography image and (b) anatomic cross-section at level of tracheal carina. Caudal view. 1, longus colli muscle (thoracic part); 2, right azygos vein; 3, esophagus: thoracic part; 4, right principal bronchus; 5, right pulmonary artery and vein; 6, right lung; 7, right atrium; 8, coronary groove; 9, sternocostal joint; 10, internal thoracic artery and vein; 11, right ventricle; 12, left coronary artery; 13, ascendens aorta; 14, left atrium; 15, left principal bronchus; 16, left pulmonary artery; 17, tracheal carina (only a); 18, left lung; 19, descendens aorta: thoracic aorta.

and abnormal structures accurately (Hounsfield, 1973; Collard et al., 1975; Barbee and Allen, 1987; Thrall, 1994; Ottesen and Moe, 1998). Radiographic exploration of the dog thorax is difficult because of its complex anatomy. The location and extent of lesions in the thorax are often difficult to define by clinical and radiographic exploration. CT soft-tissue windows are recommended to evaluate all tissues that cannot be observed by conventional radiography.

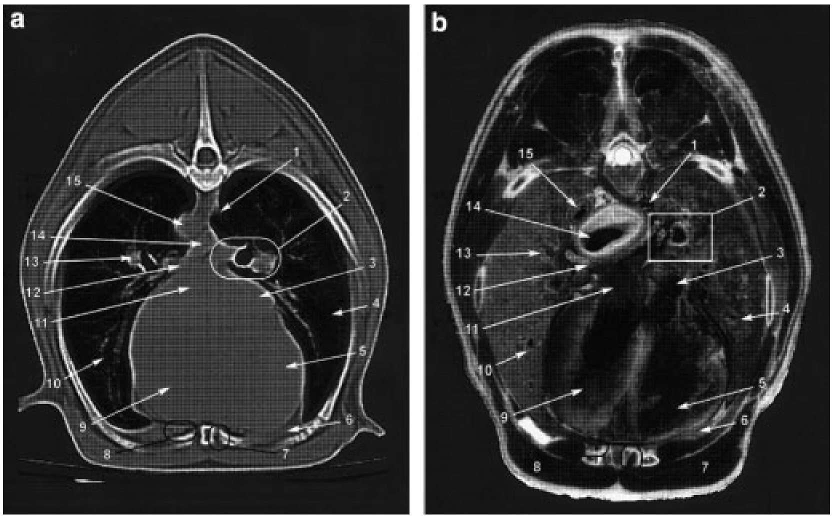

Fig. 6. (a) Computed tomography image and (b) anatomic cross-section at level of left ventricle. Caudal view. 1, right azygos vein; 2, right principal bronchus and right pulmonary artery and vein; 3, right atrium; 4, right lung; 5, right ventricle; 6, transverse thoracis muscle; 7, sternocostal joint; 8, internal thoracic artery and vein; 9, left ventricle; 10, left lung; 11, left atrium; 12, left pulmonary vein; 13, left pulmonary artery; 14, esophagus: thoracic part; 15, descendens aorta: thoracic aorta.

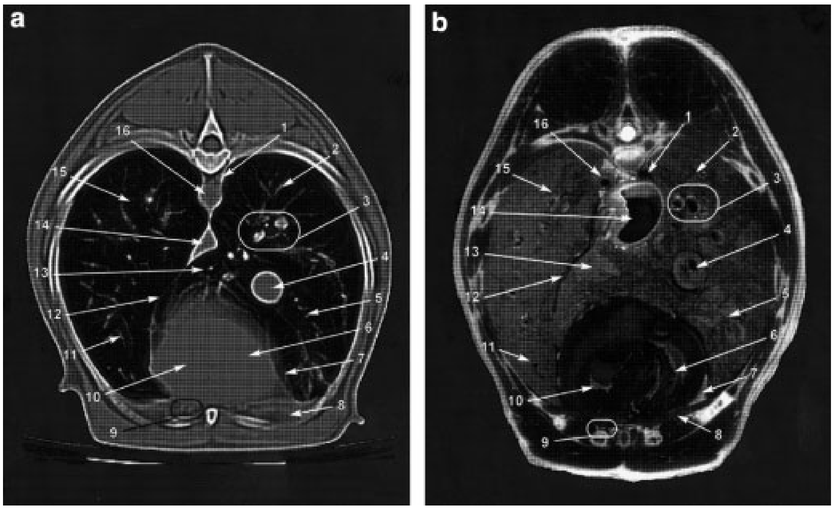

Fig. 7. (a) Computed tomography image and (b) anatomic cross-section at level of apex of heart. Caudal view. 1, right azygos vein; 2, right lung: caudal lobe; 3, lobar bronchus and right pulmonary artery and vein; 4, caudal vena cava; 5, right lung: middle lobe; 6, right ventricle; 7, pericardium and pericardial fat; 8, transverse thoracis muscle; 9, internal thoracic artery and vein; 10, left ventricle; 11, left lung: cranial lobe; 12, mediastinal pleura; 13, right lung: accessory lobe; 14, esophagus: thoracic part; 15, left lung: caudal lobe; 16, descendens aorta: thoracic aorta.

However, there are some disadvantages of CT compared with conventional radiography. Mainly, they are the high cost of the equipment and the difficult access. Anaesthesia is necessary for exploration of thorax in live animals. Adequate positioning of the patient is important to ensure a good result and anatomic symmetry of the thorax structures.

Computed tomography exploration take a relatively long time and therefore involves high radiation dosage. It has been claimed that CT scanning probably involves the highest radiation exposure per examination in the field of radiology (Ottesen and Moe, 1998).

Computed tomography images of dog thorax provided excellent detail of clinically relevant anatomy and correlated well with corresponding gross specimens. CT provides excellent spatial resolution and good discrimination between bone and soft tissue (Fike et al., 1981; Feeney et al., 1991; Thrall, 1994; Ottesen and Moe, 1998; Arencibia et al., 2000; De Rycke et al., 2003). In our study, anatomical structures of the thorax were interpreting using soft-tissue window settings. CT-soft-tissue window and cross-sections allow differentiation between soft tissues of the thorax. The planimetric or sectional anatomy of the thorax in the dog allows a correct morphologic and topographic evaluation of the anatomic structures, which is a useful tool for the identification of the CT images. The anatomic relationships were appreciated easily in the CT transverse planes.

Although the use of CT imaging in dog medicine is currently limited because its expense, availability, and the logistical problems of acquiring CT images, with developing technology, CT imaging for pets is more readily available now. In the same way, we consider it quite useful to be able to establish some references on thorax, in order to scan only selected parts during a clinical or experimental applications. Last decade several works in dogs about thorax anatomy using CT were published (Feeney et al., 1991; Smallwood and George, 1993; Assheuer and Sager, 1997). But to our knowledge none of the published works have applied and compared CT images with vascular injected anatomical cross sections. The planimetric anatomy of the thoracic cavity of the dog with vascular injection allows a correct morphological and topographic evaluation of the anatomical structures. Systemic veins and pulmonary arteries were filled with blue latex and systemic arteries and pulmonary veins with red latex so that it was a very useful tool for detailed anatomy of the pulmonary vessels and the heart base. Besides, high quality image allows a good and easy interpretation of anatomical structures of thorax cavity.

The information presented in this paper should serve as a new reference to evaluate CT images of the dog thorax and to assist interpretation of lesions of this region, particularly about blood vessels, heart and lungs.

References

Arencibia, A., J. M. Vázquez, M. Rivero, R. Latorre, J. A. Sandoval, J. M. Vilar, and J. A. Ramírez, 2000: Computed tomography of normal cranioencephalic structures in two horses. Anat. Histol. Embryol. **29,** 295–299.

Assheuer, J., and M. Sager, 1997: Thorax. In: MRI and CT Atlas of the Dog. 1st edn. Berlin and Oxford: Blackwell Science Ltd.

Barbee, D. D., and J. R. Allen, 1987: Computed tomography in the horse: general principles and clinical applications. Proc. Am. Ass Equine Pract. **32,** 483–493.

Barthez, P. Y., D. Begon, and F. Delisle, 1998: Effect of contrast medium dose and image acquisition timing on ureteral opacification in the normal dog as assessed by computed tomography. Vet. Radiol. Ultrasound **39,** 524–527.

Boyd, J. S., and C. Paterson, 1991: A Colour Atlas of Clinical Anatomy of the Dog and Cat, 1st edn. England: Wolfe Publishing Ltd.

Burk, R. L., 1991: Computed tomography of thoracic diseases in dogs. J. Am. Vet. Med. Assoc. **199,** 617–621.

Carpenter, L. G., P. D. Schwarz, J. E. Lowry, R. D. Park, and P. F. Steyn, 1993: Comparison of radiologic imaging techniques for diagnosis of fragmented medial coronoid process of the cubital joint in dogs. J. Am. Vet. Med. Assoc. **3,** 78–83.

Collard, M., H. Dupont, and G. Noel, 1975: Ere nouvelle de la neuroradiologie: la tomographie axiale tranverse computérisée-T.A.T.C. (Emi-Scanner) et ses indications. J. Radiol. **56,** 453–469.

De Rycke, L. M., J. H. Saunders, I. M. Gielen, H. J. Van Bree, and P. J. Simoens, 2003: Magnetic resonance imaging, computed tomography, and cross-sectional views of the anatomy of normal nasal cavities and paranasal sinuses in mesaticephalic dogs. Am. J. Vet. Res. **64,** 1093–1098.

Done, S. H., P. C. Goody, S. A. Evans, and N. C. Stickland, 1997. Atlas en Color de Anatomía Veterinaria. El Perro y el Gato, 1st edn. Madrid: Harcourt Brace.

Dyce, K. M., W. O. Sack, and C. J. Wensing, 1999: Anatomía Veterinaria, 2nd edn. Madrid: McGraw-Hill Interamericana.

Feeney, D., T. Fletcher, and R. Hardy, 1991: Atlas of Correlative Imaging Anatomy of the Normal Dog: Ultrasound and Computed Tomography, 1st edn. Philadelphia: WB Saunders Co.

Feeney, D., P. Evers, T. Fletcher, R. Hardy, and L. Wallace, 1996: Computed tomography of the normal canine lumbosacral spine: a morphological perspective. Vet. Radiol. Ultrasound **37,** 399–411.

Fike, J. R., R. A. LeCouteur, and C. E. Cann, 1981: Anatomy of the canine brain using high resolution computed tomography. Vet. Radiol. **22,** 236–243.

Hounsfield, G. N., 1973: Computerized transverse axial scanning (tomography). Br. J. Radiol. **46,** 1016.

Nickel, R., A. Schummer, E. Seiferle, and W. O. Sack, 1979: The Viscera of the Domestic Mammals, 2nd edn. Berlin-Hamburg: Verlag Paul Parey.

Nickel, R., A. Schummer, and E. Seiferle, 1981: The circulatory system, the skin and the cutaneous organs of the domestic mammals. In: The Anatomy of the Domestic Animals. vol. 3, 1st edn. Berlín: Verlag Paul Parey.

Ottesen, N., and L. Moe, 1998: An introduction to computed tomography (CT) in the dog. Eur. J. Compan. Anim. Pract. **8,** 29–36.

Ruberte, J., and J. Sautet, 1996. Atlas de Anatomía del Perro y del Gato. Vol. 2: tórax y miembro torácico, 1st edn. Barcelona: Multimédica.

Samii, V., D. Biller, and P. Koblik, 1998: Normal cross-sectional anatomy of the feline thorax and abdomen: comparison of computed tomography and cadaver anatomy. Vet. Radiol. Ultrasound **39,** 504–511.

Schaller, O., 1992: Illustrated Veterinary Anatomical Nomenclature. Stuttgart: Ferdinand Enke Verlag.

Schwarz, L. A., and A. S. Tidwell, 1999: Alternative imaging of the lung. Clin. Tech. Small Anim. Pract. **14,** 187–206.

Smallwood, J. E., and T. F. George, 1993: Anatomic atlas for computed tomography in the mesaticephalic dog: thorax and cranial abdomen. Vet. Radiol. Ultrasound **34,** 65–83.

Spann, D. R., R. K. Sellon, D. E. Thrall, A. E. Bostian, and G. T. Boston, 1998: Computed tomographic diagnosis: use of computed tomography to distinguish a pulmonary mass from alveolar disease. Vet. Radiol. Ultrasound **39,** 532–535.

Thrall, D. E., 1994: Textbook of Veterinary Diagnostic Radiology. Philadelphia: W. B. Saunders Co.

Vázquez, J. M., G. Ramírez, F. Gil, R. Latorre, F. Moreno, O. López, M. Orenes, and A. Arencibia, 2000: Atlas de Anatomía Clínica. Perro y gato. Cavidades torácica, abdominal y pelviana, 1st edn. Murcia: AG Novograf SA.

Waters, D. J., F. V. Coakley, M. D. Cohen, M. M. Davis, B. Karmazyn, R. Gonin, M. P. Hanna, D. W. Knapp, and S. A. Heifetz, 1998: The detection of pulmonary metastases by helical CT: a clinicopathologic study in dogs. J. Comput. Assist. Tomogr. **22,** 235–240.